JOURNAL OF MATERIALS SCIENCE **34** (1999) 2345–2349

Deformation mechanisms in the γ-TiAl phase present in the Ti-46Al-2V-0.4Er alloy

K. DAS, S. DAS
Department of Metallurgical and Materials Engineering, Indian Institute of Technology, Kharagpur-721 302, India
E-mail: sdas@hijli.iitkgp.ernet.in

Deformation microstructures of the γ-TiAl Phase in two-phase ($\alpha_2 + \gamma$) alloy, Ti-46Al-2V-0.4Er (all compositions are given in atomic percent), have been studied by transmission electron microscopy. Heat treated samples of this alloy were subjected to 3% plastic strain in compression at room temperature, 600 °C, and 900 °C. Majority of dislocations present in the as heat treated and deformed samples are of $\mathbf{b} = 1/2 < 110]$ type. Formation of loops from the dislocations are also observed. Isolated super dislocations and faulted dipoles are seldom seen in the microstructures. Plenty of twins are present in these samples and it appears that their density increases with increasing deformation temperature. The deformation microstructures of the alloy studied here are quite similar to those in the binary two-phase titanium aluminides or the V containing two-phase titanium aluminides. It appears that Er does not significantly change the deformation microstructure of this two-phase alloy, although Er has a significant effect on the deformation microstructure of the single-phase γ-TiAl alloys. © *1999 Kluwer Academic Publishers*

1. Introduction

The deformation microstructures of γ-TiAl consist of $\mathbf{b} = 1/2$ [110] type dislocations, $\mathbf{b} = [011]$ type superdislocations, and [112] $(1\,1\,\bar{1})$ type twins [1, 2]. The anisotropy of the charge density distribution near the Ti atoms in the γ-TiAl unit cell may cause many valleyed Peierls relief, and thus may affect the dislocation mobility [3]. Following the work of Greenberg *et al.* [3], Court *et al.* [4] suggest that the $1/2 < 110]\{111\}$ type slip system is basically sessile at room temperature owing to the covalency effect. The increased activity of this type of slip system at 600 °C is probably due to the decrease in Peierls stress caused by thermal activation which might have resulted in the increased ductility of γ-TiAl at elevated temperature. The two-phase alloys are more ductile at room temperature than the single-phase alloys. The room temperature deformation microstructure of the γ-TiAl phase in a two phase Ti-46Al alloy is dominated by the $\mathbf{b} = 1/2 < 110]$ type dislocations [5]. In contrast, this dislocation experiences a very high Peierls stress in a single-phase alloy owing to the directionality of bonds between the Ti atoms. These authors [5] concluded that the increased mobility of $\mathbf{b} = 1/2 < 110]$ type dislocations at room temperature in the two-phase alloys is due to the removal of interstitial impurities from the γ-TiAl phase by α_2-Ti_3Al, acting as a getter; which in turn reduces the degree of directionality of bonding between the Ti atoms.

The beneficial effect of V addition on the room temperature ductility of both single-phase and two-phase alloys has been the subject of few published papers [6–9]. After studying the deformation microstructures of the γ-TiAl phase in the Ti-52Al-3V and Ti-46Al-2V alloys, the present authors concluded that the deformation microstructures of the ternary alloys are quite similar to their binary counterparts [10, 11]. The effect of Er on the room temperature deformation microstructure of single-phase γ-TiAl has been studied by Vasudevan *et al.* [12]. It was found by these authors that during room temperature deformation dislocations with $\mathbf{b} = 1/2 < 110]$, having an increased mobility, contributed most significantly to plastic strain owing to a reduction in the directionality of the bonding charge densities due to the gettering of interstitial impurities by Er. The present note reports the results of experiments involving the deformation of samples of Ti-46Al-2V-0.4Er, which permits to study the effect of Er on the deformation behaviour of V containing two-phase alloy.

2. Experimental

Master ingots of Ti-46Al-2V-0.4Er (at %) alloy was prepared by non-consumable electrode arc melting technique in a water-cooled copper hearth under an inert atmosphere of Ar using high purity Ti (99.9%), Al (99.999%), V (99.9%) and Er (99.95%) (all with respect to metallic elements). Ingots were heat treated in a vacuum furnace at 1250 °C for 12 hours and then furnace cooled to room temperature very slowly. Compression coupons of dimensions $5 \times 5 \times 12.5$ mm were machined from these heat-treated materials and then were subjected to true strains of 3% in compression at room temperature, 600 °C and 900 °C.

Thin slices of deformed samples were cut parallel to the compression axis and discs of 3 mm diameter were punched from these thin slices. Transmission electron microscopy (TEM) specimens were prepared from those discs by using twin-jet electropolishing technique using 8 vol % sulphuric acid in methanol at operating conditions of 50 V, 70 mA and $-40\,^{\circ}$C. The thin foils were examined in a Philips CM12 transmission electron microscope operating at 120 kV.

3. Results

3.1. Microstructure of as heat treated samples

The nature of the dislocations present in these samples has been characterized by diffraction contrast experiments in the transmission electron microscope and an example is given in Fig. 1a. There are two types of dislocations, labeled as A and B, present in the as heat treated microstructure. Both types of dislocations are in contrast when imaged with $\mathbf{g} = 1\,1\,1$ (Fig. 1a) and $\mathbf{g} = \bar{1}\,1\,1$; $\mathbf{g}$ is the reciprocal lattice vector of the reflecting planes. Dislocation A is not in contrast when imaged with either $\mathbf{g} = 2\,\bar{2}\,0$ (Fig. 1b) or $\mathbf{g} = \bar{3}\,1\,\bar{1}$. Similarly B type dislocations are not in contrast when imaged with $\mathbf{g} = 0\,0\,\bar{2}$ (Fig. 1c) and give residual contrast when imaged with $\mathbf{g} = 1\,1\,\bar{1}$. From this analysis the Burgers vector have been determined as $\mathbf{b} = 1/2\,[1\,1\,\bar{2}]$ for dislocation A and $\mathbf{b} = 1/2\,[1\,1\,0]$ for B type dislocations. From trace analysis it has been revealed that line direction of dislocation A is close to $[\bar{1}\,\bar{1}\,2]$, whereas line directions of B type dislocations are close to $[\bar{1}\,0\,\bar{1}]$. Therefore, dislocation A is pure screw lying on (111) and B type dislocations are mixed lying on $(1\,1\,\bar{1})$.

3.2. Microstructure of sample deformed at room temperature

Fig. 2a shows a typical deformation microstructure of this sample when imaged with $\mathbf{g} = 2\,0\,0$. The dislocations are labeled as A and B. Type A dislocations are not in contrast when imaged with $\mathbf{g} = 1\,1\,\bar{1}$ and $\mathbf{g} = 2\,2\,0$, yielding a Burgers vector given by $\mathbf{b} = 1/2[1\,1\,0]$. Similarly type B dislocations are out of contrast when imaged with $\mathbf{g} = 1\,1\,1$ and $\mathbf{g} = 1\,\bar{3}\,1$, yielding a Burgers vector given by $\mathbf{b} = [1\,0\,1]$. Trace analysis reveals that type A dislocations are pure screw lying on $(1\,1\,\bar{1})$ and type B are mixed lying on $(1\,1\,1)$. Twins and very few faulted dipoles are also present in the deformed sample.

3.3. Microstructure of sample deformed at 600 °C

The density of dislocations in the sample deformed at 600 °C changes markedly; large number of curved dislocations are also observed. A typical deformation micrograph is presented in Fig. 2b, which has been imaged with $g = 2\,2\,0$. Dislocations labeled as A, B, C and D are visible in this micrograph. They are also in contrast when imaged with $g = 1\,1\,\bar{1}$. They are out of contrast when imaged with $g = 1\,1\,1$ and yield residual contrast with $g = 0\,0\,2$. From this analysis the Burgers vector have been determined to be $1/2[1\,1\,0]$. Trace analysis reveals that these dislocations are mixed dislocations lying on {111} type slip planes. The $\mathbf{b} = 1/2 < 110]$ dislocations are generally curved and formation of loops from these dislocations is clearly evident in the microgrph. This sample has also significant number of twins.

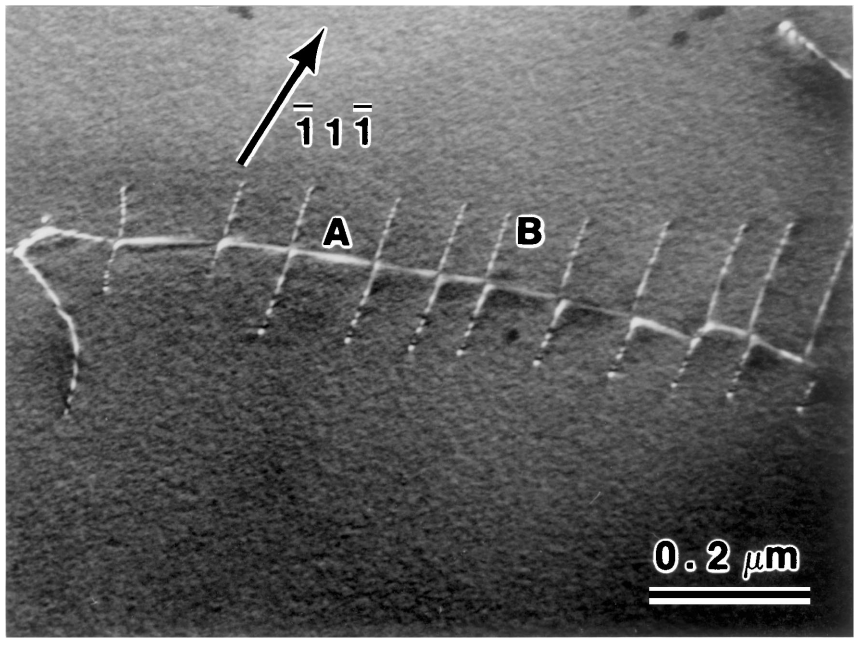

(a)

Figure 1 (a-c) Weak-beam dark-field transmission electron micrographs obtained from the γ-TiAl phase present in the as heat treated Ti-46Al-2V-0.4Er alloy (*Continued*).

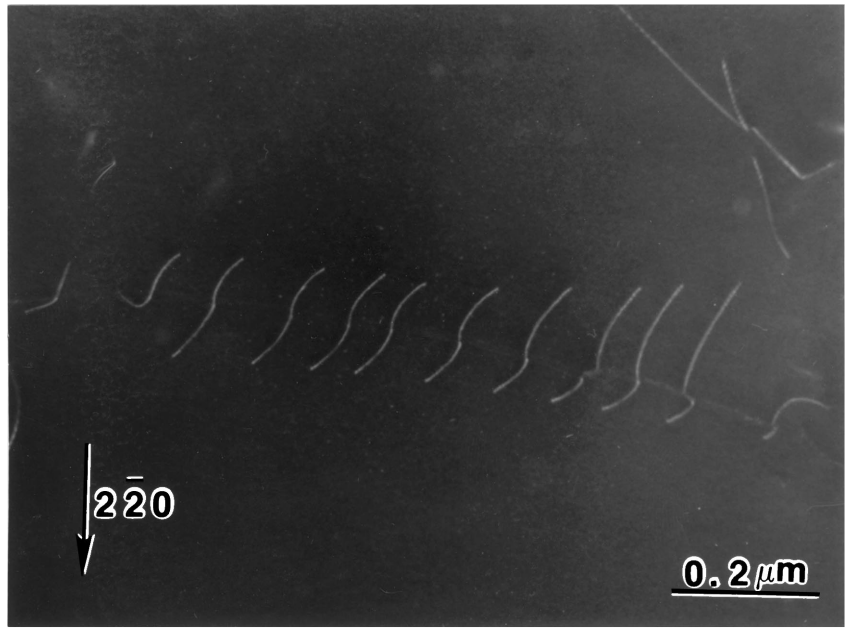

(b)

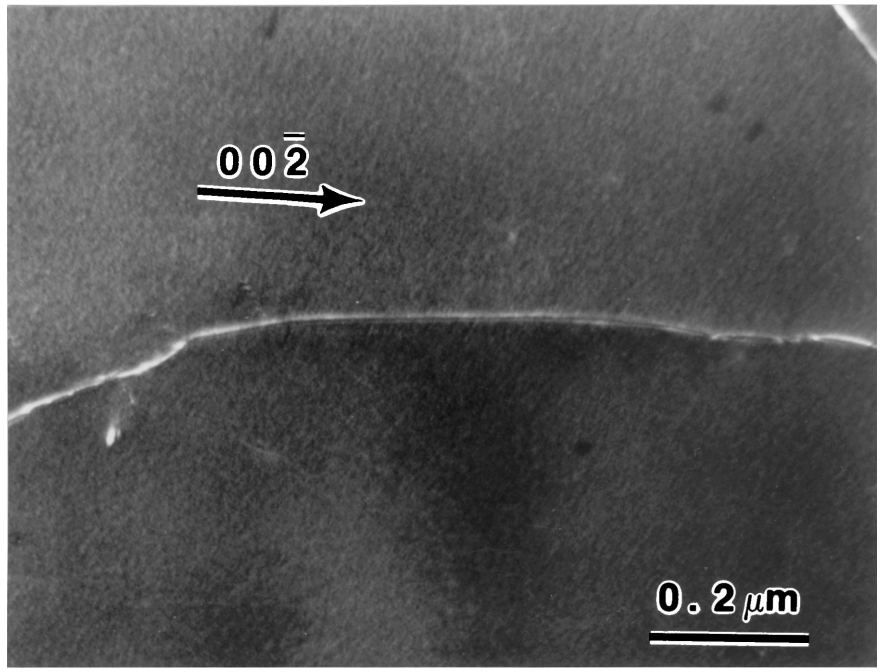

(c)

Figure 1 (*Continued*).

3.4. Microstructure of sample deformed at 900 °C

The 900 °C deformation microstructure is shown in Fig. 2c, imaged with $g = 1\,\bar{1}\,1$. They are also in contrast when imaged with $g = 0\,2\,\underline{0}$. They yield residual contrast when imaged with $g = 1\,\bar{1}\,1$, but they are completely invisible when imaged with $g = 0\,0\,2$. Therefore, the Burgers vector of this type of dislocations is $1/2[1\,\bar{1}\,0]$, and they are lying on $(1\,\bar{1}\,1)$ slip plane. Some of these dislocations lie close to the edge orientation and some of them are of mixed type. Twins and dislocation loops can also be seen in this sample.

4. Discussion

The present study shows that in samples of Ti-46Al-2V-0.4Er deformation is accomplished predominantly by glide of dislocations with $\mathbf{b} = 1/2 < 110]$. Dislocation loops can also be seen in the elevated temperature deformation microstructures, and they are associated with the $\mathbf{b} = 1/2 < 110]$ curved and tangled dislocations. They most likely form due to the interactions of the $\mathbf{b} = 1/2 < 110]$ dislocations. Such dislocation morphology has resulted from cross slip, and might be responsible for high temperature hardening. The deformation microstructure of Ti-52Al-0.4Er was evaluated by Aindow *et al*. [13]. The room temperature deformation microstructure is dominated by $\mathbf{b} = 1/2 < 110]$ type dislocation. In contrast, the room temperature deformation microstructure of Ti-52Al is dominated by $\mathbf{b} = <101]$ type dislocation, and very few $\mathbf{b} = 1/2 < 110]$ type dislocations are present in the sample. When Er is added, interstitial impurities are

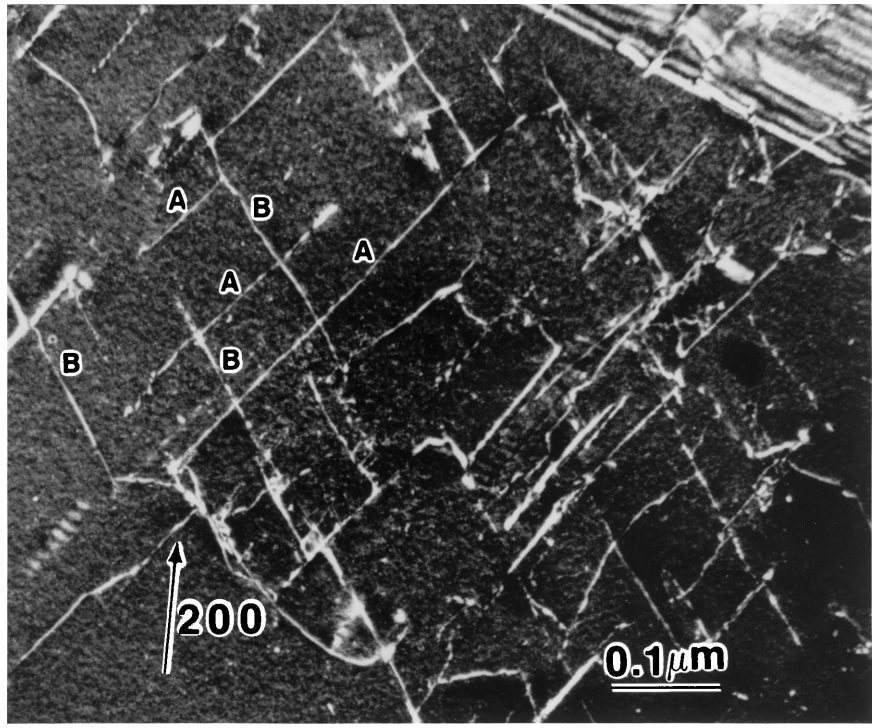

Figure 2a Weak-beam dark-field transmission electron micrograph obtained from the γ-TiAl phase present in the Ti-46Al-2V-0.4Er alloy deformed in compression at room temperature.

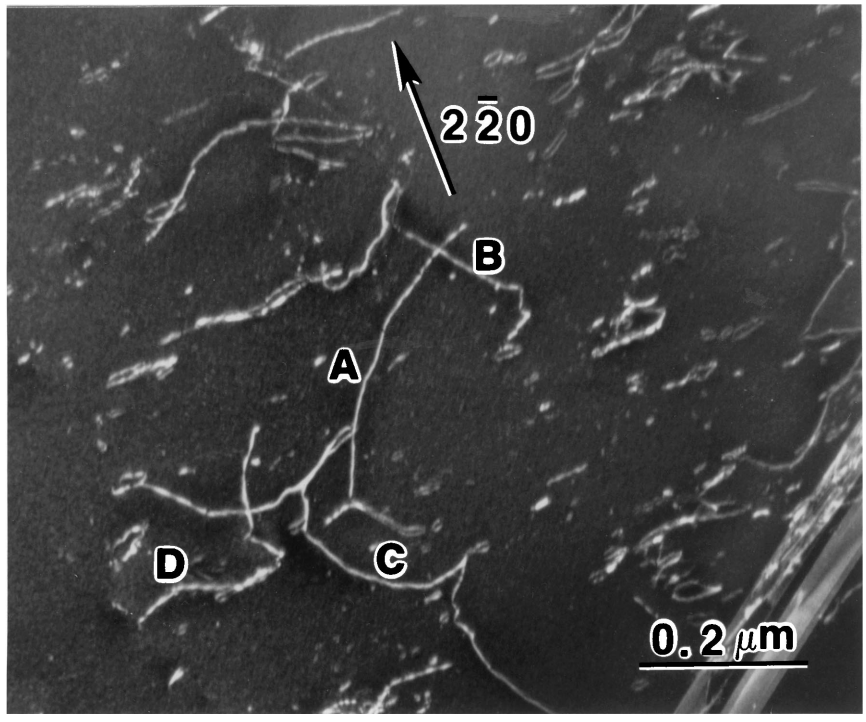

Figure 2b Weak-beam dark-field transmission electron micrograph obtained from the γ-TiAl phase present in the Ti-46Al-2V-0.4Er alloy deformed in compression at 600 °C.

removed from the γ-phase by the gettering action of Er, and thus Er_2O_3 particles are formed. The decrease in amount of interstitials reduces the degree of directionality of bonding between the Ti atoms, which in turn decreases the anisotropy in Peierls stress. The dislocations $\mathbf{b} = 1/2 < 110]$ lie in the deep Peierls valley in Ti-52Al alloy, whereas these dislocations do not lie in deep Peierls valley in Ti-52Al-0.4Er alloy owing to the removal of interstitial impurities from the γ-TiAl phase by the gettering effect of Er.

In the present study, it is expected that Er will remove interstitial impurities from the matrix in a similar manner as discussed above. Indeed examination of the microstructure revealed a dispersion of particles of Er_2O_3, presumably containing N and C, since particles of $Ti_2Al(C, N)$ were not observed, as in the case of binary alloys. Interstitial impurities will also be removed from the γ-TiAl phase by α_2-Ti_3Al, acting as a getter in the two-phase alloy Ti-46Al-2V-0.4Er. Therefore, it is expected that the removal of impurities from γ-TiAl

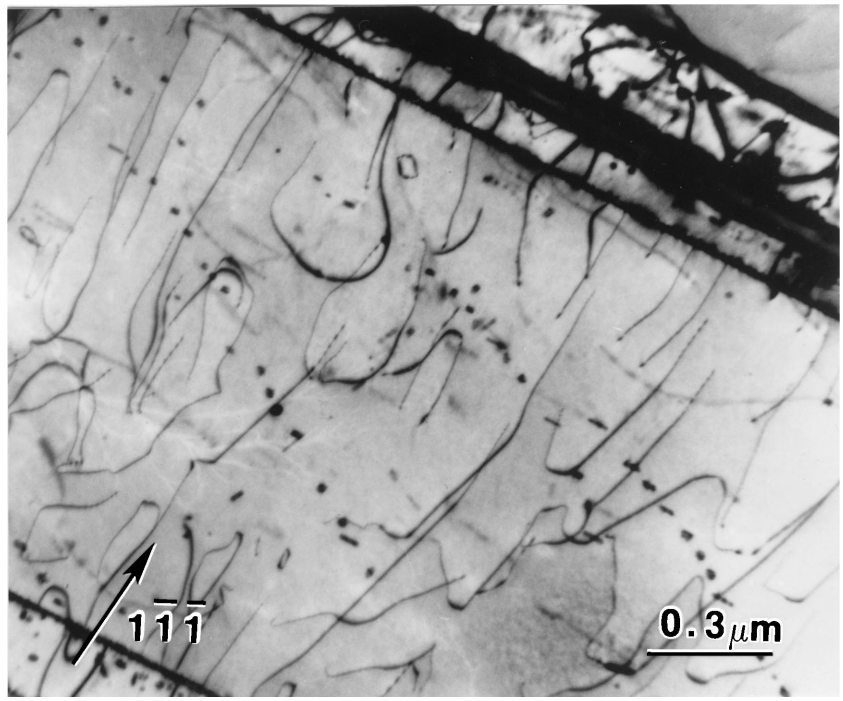

Figure 2c Bright-field transmission electron micrograph obtained from the γ-TiAl phase present in the Ti-46Al-2V-0.4Er alloy deformed in compression at 900 °C.

by the gettering effect of both Er and α_2-Ti_3Al will result in a very pure γ-TiAl matrix, which in turn will reduce the degree of directionality of bonding between Ti atoms. This in turn will cause the increased mobility of $\mathbf{b} = 1/2 < 110]$ dislocation. If the deformation microstructures of Ti-46Al-2V alloy [11] and Ti-46Al-2V-0.4Er alloy are compared, it can be seen that they are very similar. Therefore, this study can not confirm whether Er has an added advantage in improving ductility of a two-phase alloy. It should be noted that although in the presence of Er_2O_3 particles, the increased mobility of various dislocations may imply improved ductility, other factors such as cleavage stress may be exacerbated by the high value of yield stress exhibited by these Er_2O_3 containing fine grained samples.

5. Summary

Majority of dislocations present in samples deformed at various temperatures are of $\mathbf{b} = 1/2 < 110]$ type. The number of $\mathbf{b} = <101]$ superdislocation at high temperature is quite low, and this is probably owing to their low mobility caused by the formation of Kear-Wilsdorf [14] type of locks. Dislocation loops can also be seen in the elevated temperature deformation microstructure, and they are associated with the $\mathbf{b} = 1/2 < 110]$ curved and tangled dislocations. The density of twins in the samples is quite high, and it appears to increase with the increasing deformation temperature. The deformation microstructures of the alloys studied here are quite similar to those observed in the binary two-phase titanium aluminides or the V containing two-phase titanium aluminides, and it appears that Er does not significantly change the deformation microstructures of this two-phase alloy, although Er has a significant effect on the deformation microstructure of the single-phase alloy.

References

1. D. SCHECHTMAN, M. J. BLACKBURN and H. A. LIPSITT, *Metall. Trans.* **5** (1974) 1373.
2. H. A. LIPSITT, D. SCHECHTMAN and R. E. SCHAFRIK, *Metall. Trans. A* **6** (1975) 1991.
3. B. A. GREENBERG, V. I. ANISIMOV, YU. N. GORNOSTIREV and G. G. TALUTS, *Scripta Metall.* **22** (1988) 859.
4. S. A. COURT, V. K. VASUDEVAN and H. L. FRASER, *Phil. Mag.* **61** (1990) 141.
5. V. K. VASUDEVAN, M. A. STUCKE, S. A. COURT and H. L. FRASER, *Phil. Mag. Lett.* **59** (1989) 299.
6. R. L. FLEISCHER, D. M. DIMIDUK and H. A. LIPSITT, *Annu. Rev. Mater. Sci.* **19** (1989) 231.
7. M. J. BLACKBURN and M. P. SMITH, AFML-TR-78-78, Air Force Mat. Lab., Wright-Patterson AFB, OH, USA, 1978.
8. S. H. WHANG and Y. D. HAHN, in "High Temperature Ordered Intermetallic Alloys III," Vol. 133, MRS Symp. Proc., edited by C. T. Liu, A. I. Taub, N. S. Stoloff and C. C. Koch (MRS, Pittsburgh, PA, Materials Research Society, 1989), p. 687.
9. E. L. HALL and S. C. HUANG, in "High Temperature Ordered Intermetallic Alloys III," Vol. 133, MRS Symp. Proc., edited by C. T. Liu, A. I. Taub, N. S. Stoloff and C. C. Koch (MRS, Pittsburgh, PA, Materials Research Society, 1989) p. 693.
10. K. CHAUDHURI and S. DAS, *Phil. Mag. Lett.* **67** (1993) 143.
11. S. DAS and K. CHAUDHURI, *Scripta Metall. et Materialia* **32** (1995) 201.
12. V. K. VASUDEVAN, S. A. COURT, P. KURATH and H. L. FRASER, *Scripta Metall.* **23** (1989) 907.
13. M. AINDOW, K. CHAUDHURI, S. DAS and H. L. FRASER, *ibid.* **24** (1990) 1105.
14. B. H. KEAR and H. G. E. WILSDORF, *Trans. Metall. Soc. AIME* **224** (1962) 382.

Received 20 October
and accepted 16 November 1998